Supporting Information

Highly efficient sky-blue perovskite light-emitting diode via suppressing non-radiative energy loss

Zhaohua Zhu[1,2], Yan Wu[1,2], Yang Shen[4], Jihua Tan[1,2], Dong Shen[1,2], Ming-Fai Lo[3], Menglin Li[2,3], Yi Yuan[3], Jian-Xin Tang[4], Wenjun Zhang[2,3], Sai-Wing Tsang[2,3], Zhiqiang Guan[1,2,3], Chun-Sing Lee[1,2*]*

[1]Department of Chemistry, City University of Hong Kong, Kowloon 999077, Hong Kong SAR, P. R. China

[2]Center of Super-Diamond and Advanced Films (COSDAF), City University of Hong Kong, Kowloon, Hong Kong SAR 999077, P. R. China

[3]Department of Material Science and Engineering, City University of Hong Kong, Kowloon 999077, Hong Kong SAR, P. R. China

[4]Institute of Functional Nano and Soft Materials (FUNSOM), Jiangsu Key Laboratory for Carbon-Based Functional Materials and Devices, Soochow University, Suzhou 215123, Jiangsu, China

[*]Corresponding author

Email: zqguan2@cityu.edu.hk**;** apcslee@cityu.edu.hk

Supplementary Note

1. Charge-modulated electroabsorption spectroscopy (CMEAS)

CMEAS is a technique that can record charge-transfer process[1]. When a charge-transfer process occurs (for example, an electron transfers from inorganic cluster to organic ligand), a hole will leave in the inorganic cluster. Under a modulated electric field, the separated charges (electron or hole) experience a trapping/de-trapping process, which slows down the response to the modulated field. This is different from the situation of excitonic transition states, who can response extremely fast to the modulated field and thus generate a strong in-phase signal. The charge-transfer process, on the contrary, leads to obvious quadrature signals.

Another evidence for the occurrence of triplet-triplet energy transfer is the different response to the varied DC biases between excitonic state and charge-transfer state. The EA signal of excitonic state can be expressed as Stark effect, where EA

signal is proportional to the build-in potential[2]. On the other hand, charge-transfer states show a DC voltage independent feature, which does not follow Stark effect[1]. The CMEAS signal of DC voltage dependence is shown in **Figure S15** (Supporting Information). For the signals of PEACl-based perovskite excited at 3.2 eV, a DC voltage independent feature can be found, proving that the triplet-triplet Dexter electron-transfer occurs at this energy level. Whereas for the signals of 3.6 eV, a high energy vibrational excitonic state, a slowly decrease with increasing DC voltage can be observed, accompanied with a sudden rise appeared at 2.5 V. The inflection represents the directional change of build-in potential. The DC voltage dependent experiments were also carried out for $EDBECl_2$-based perovskite aiming to provide more evidence. Signals excited at 2.5 eV and 3.54 eV are exhibited. Both of them show the feature of excitonic states, demonstrating that no triplet-triplet electron-transfer happens.

2. Calculation on density of trap states for holes and electrons

Single carrier devices are used for calculating the density of trap states. The structure of hole-only device (HOD) is ITO/PEDOT:PSS/PVK/PFI/perovskite/TFB (30

nm)/MoO_3 (10 nm)/Ag (100 nm), where TFB is poly [(9,9-dioctylfluorenyl-2,7-diyl)-co-(4,40-(N-(p-butylphenyl))- diphenylamine)]. The structure of electron-only device (EOD) is ITO/ZnO (40 nm)/perovskite/TPBi/LiF/Al. The J-V curve of single carrier devices can be divided into three regions in log-log graph, i.e. the Ohmic region at low voltage (n=1, where n is the slope), the trap-filled limit region (n>3) and space-charge-limited current regime (n=2). A trap-filled limit voltage (V_{TFL}) is defined as the crossover point between Ohmic and trap-filled limit regions, which means all the traps are filled with carriers[3]. The densities of hole and electron traps can be calculated via an equation of

$$n_{t(e/h)} = 2\varepsilon\varepsilon_0 V_{TFL(e/h)} / \left(ed^2\right) \quad (1)$$

where $n_{t(e/h)}$ is trap density for electron ($n_{t(e)}$) and hole ($n_{t(h)}$), respectively; ε=4.8 is relative permittivity[4], ε_0 is vacuum permittivity, e is elementary charge and d is the thickness of perovskite layer. The measured J-V curves of hole-only- and electron-only-devices are shown in **Figure S8** and **S9**, respectively. Resultant values are listed in **Table S4**.

Supplementary Figure

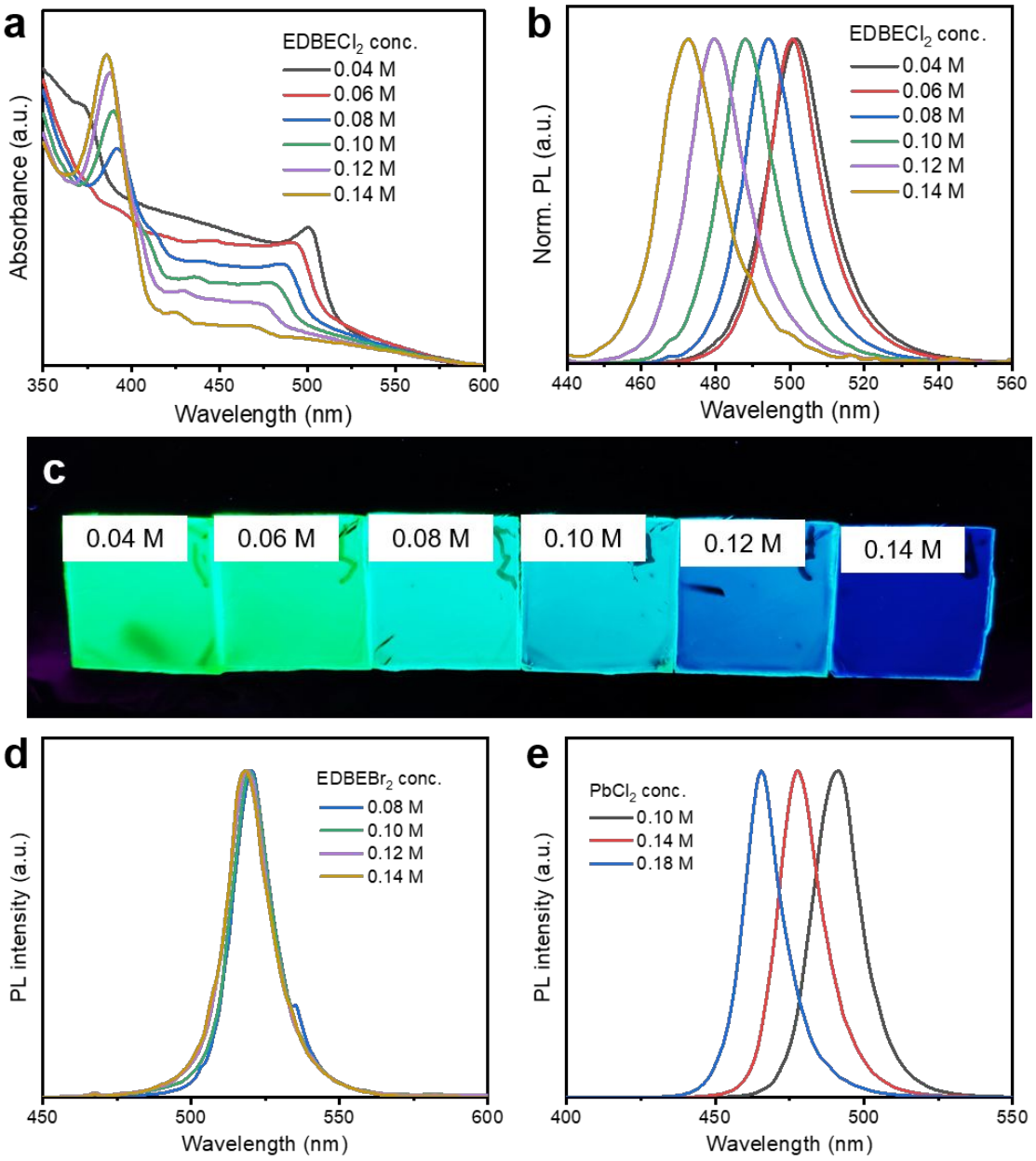

Figure S1. Spectra and photographs of perovskite films. (a) Absorption spectra of perovskite films. The 3D peak blue-shift from 501 to 467 nm and excitonic peak of n=2 phase blue-shift from 391 to 386 nm. (b) PL spectra of perovskite films. PL peaks blue-shift from 502 to 473 nm. (c) Photographs of perovskite films excited with UV light at 375 nm. Emissive colors change from green to blue with increasing the $EDBECl_2$

concentration. (d) PL spectra of perovskite films with different $EDBEBr_2$ concentration. (e) PL spectra of perovskite films with different $PbCl_2$ concentration.

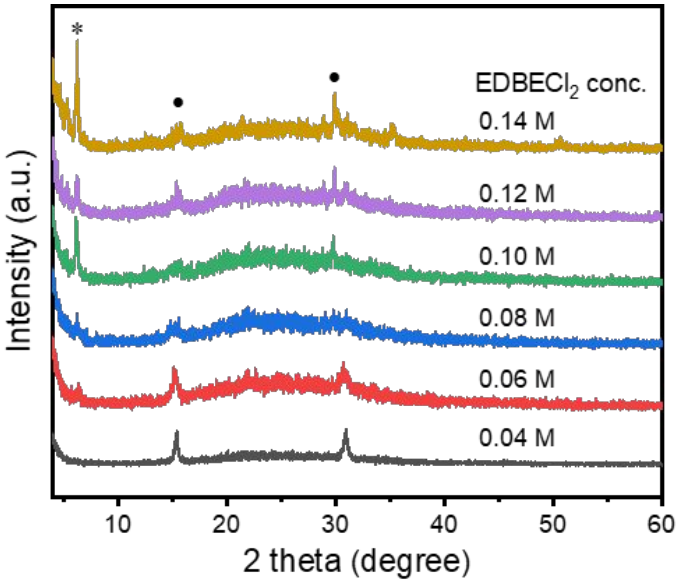

Figure S2. XRD patterns of perovskite films with different $EDBECl_2$ concentration. Peaks with asterisk (∗) belong to (020) plane of quasi-2D perovskite and peaks with circle mark (•) are from (101) and (202) planes of 3D perovskite. With increase of $EDBECl_2$ concentration, intensity of (020) peak becomes higher while (101) and (202) peaks become lower, indicating a change from 3D to 2D structure.

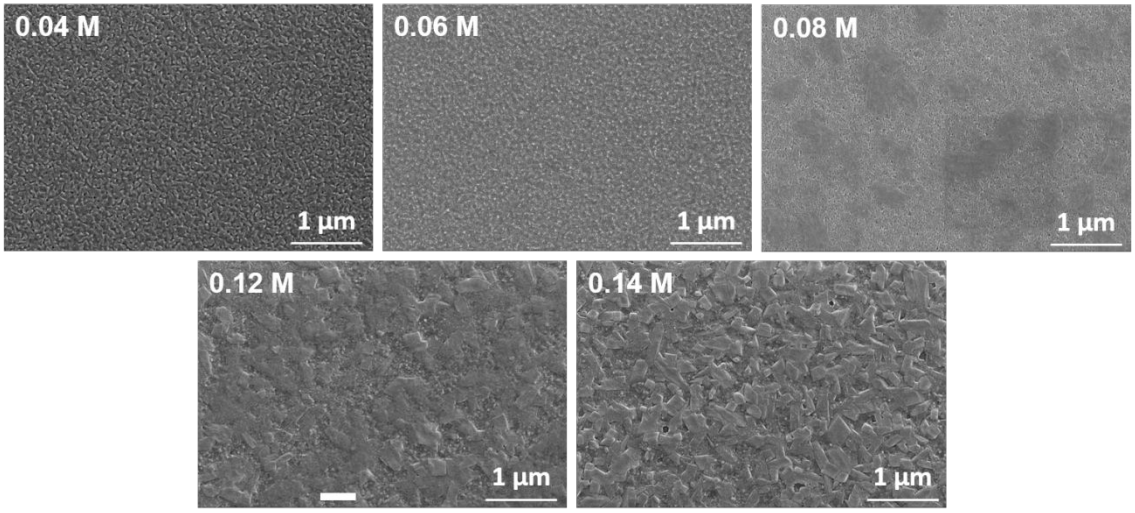

Figure S3. SEM images of the perovskite films with different $EDBECl_2$ concentration. Introducing $EDBECl_2$ can reduce perovskite crystallite size, which is a typical process in quasi-2D system. Nevertheless, too much $EDBECl_2$ leads to rough morphologies with large plate-shape 2D perovskite covering on the surface.

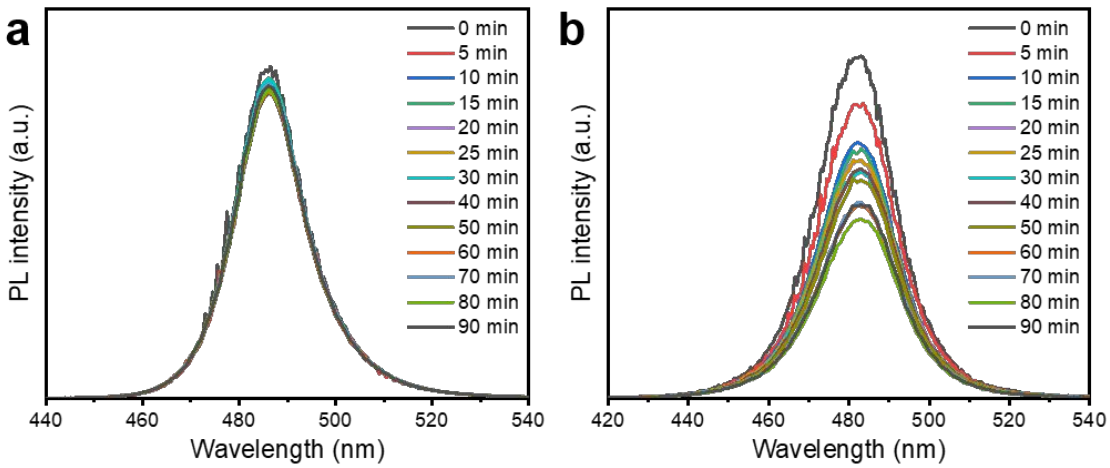

Figure S4. PL evolution of two kinds of quasi-2D perovskites with $EDBECl_2$ and PEACl through heat treatment of 60 °C. (a) PL spectra of $EDBECl_2$ perovskite. The intensity drops for only 6% after 90 min without any peak shift. (b) PL spectra of PEACl perovskite. Intensity drops for more than 50% and the red-shift of 3 nm happens after 90 min heat treatment.

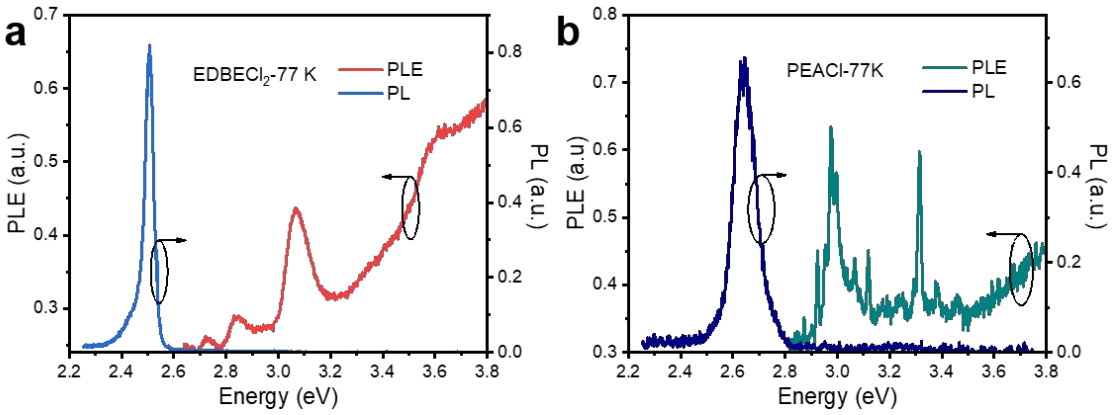

Figure S5. PLE and PL spectra measured at 77 K. (a) PLE and PL spectra of $EDBECl_2$-based perovskite. PLE spectra show the highest excitonic peak at 3.07 eV (n=2) together with a continuum band from 3.2 eV. (b) PLE and PL spectra of PEACl-based perovskite. The highest excitonic peak of n=1 is at 3.32 eV and the continuum band starts from 3.5 eV.

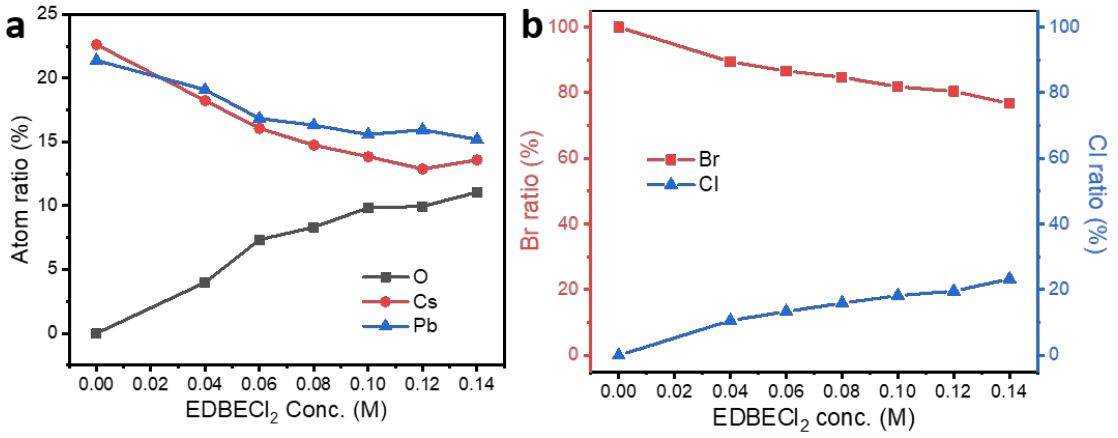

Figure S6. Statistics of atom ratio in perovskite with different $EDBECl_2$ concentrations. (a) Statistics of atom ratio of O, Cs and Pb in all elements. With increase of $EDBECl_2$ concentration, O ratio keeps rising. For the concentration of 0.1 M, a rough ratio of ligand: inorganic cluster is about 1: 3. Considering there should be an amount of $n=\infty$ phase, excess $EDBECl_2$ molecules exist outside the perovskite crystal lattice, serving as Lewis base PAs. (b) Relative statistics of atom ratio between Br and Cl. With increase of $EDBECl_2$ concentration, Cl ratio increases and Br decrease. The ratio of Cl: Br is close to 1:4 for 0.1 M $EDBECl_2$.

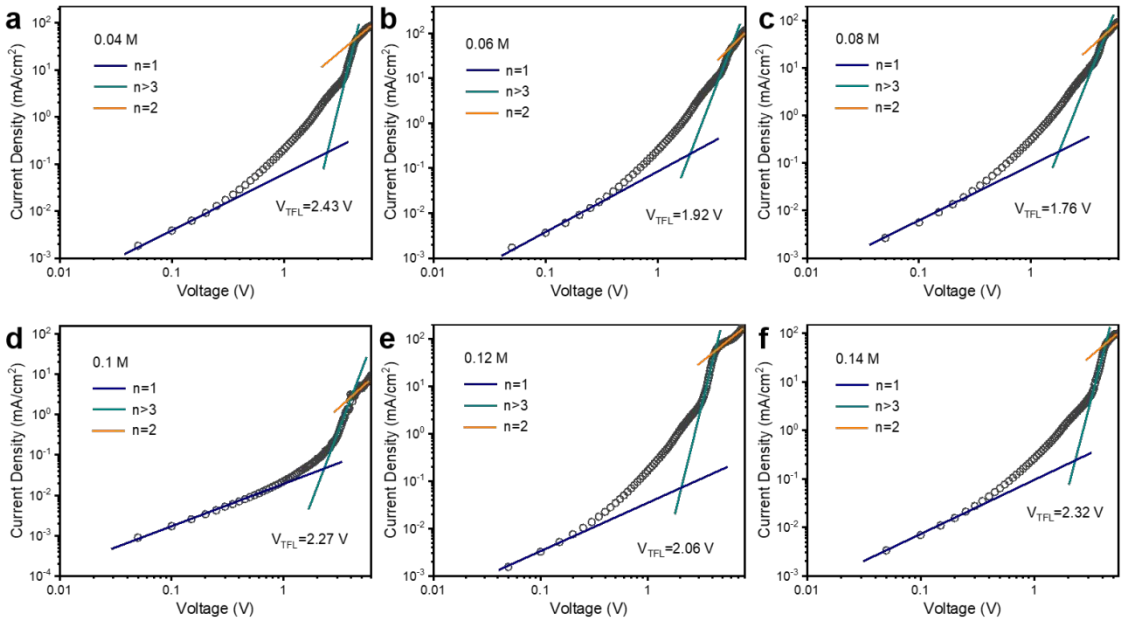

Figure S7. Current density-voltage (J-V) curves of hole-only devices with different $EDBECl_2$ concentrations.

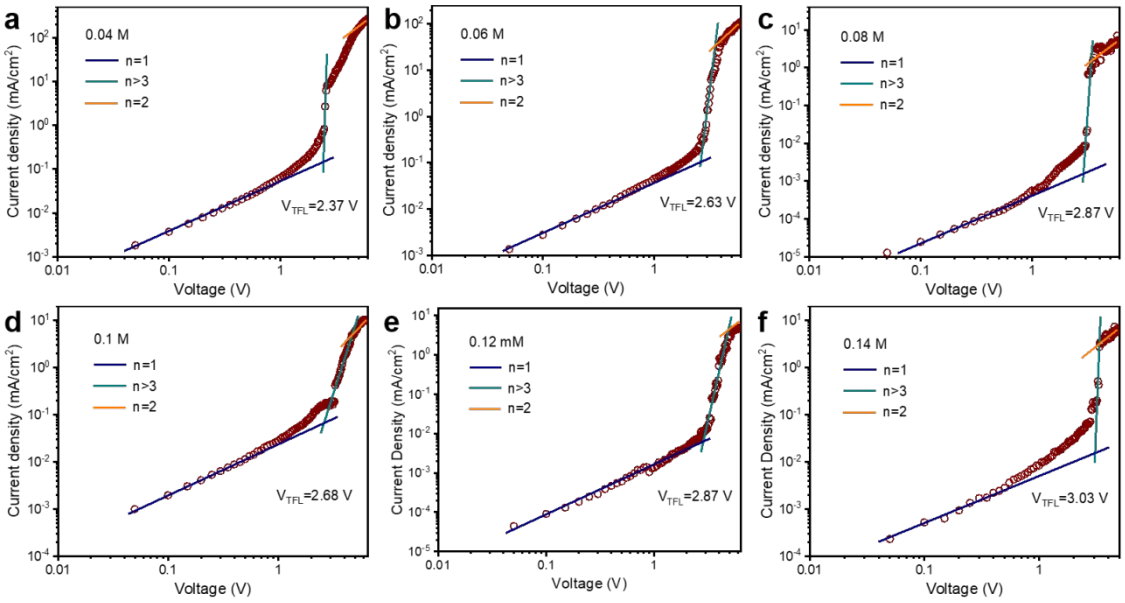

Figure S8. J-V curves of electron-only devices with different $EDBECl_2$ concentrations.

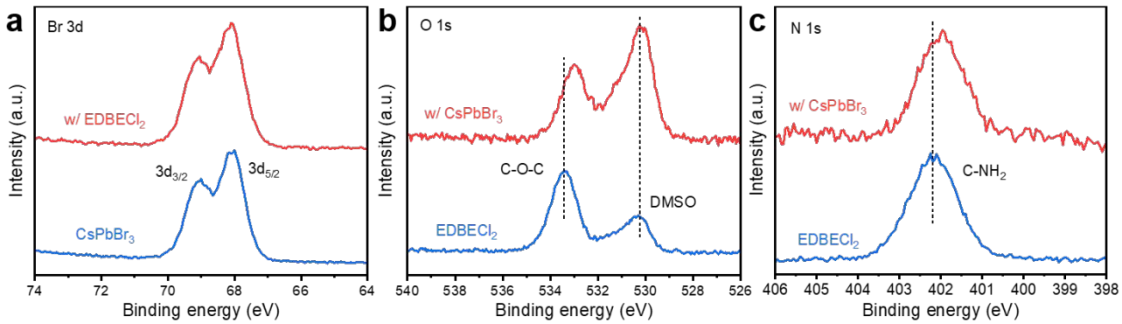

Figure S9. High resolution XPS core level spectra of perovskites with and without $EDBECl_2$. (a) Br 3d, (b) O 1s and (c) N 1s. For Br 3d peaks, $EDBECl_2$ does not change the profile of XPS spectra. However, adding ligand shifts the peaks of O 1s and N 1s to lower energy, which is opposite to the Cs 3d and Pb 4f, suggesting interactions between Cs^{+}/Pb^{2+} ions in inorganic layers and C-O-C/-NH_2 groups in $EDBECl_2$.

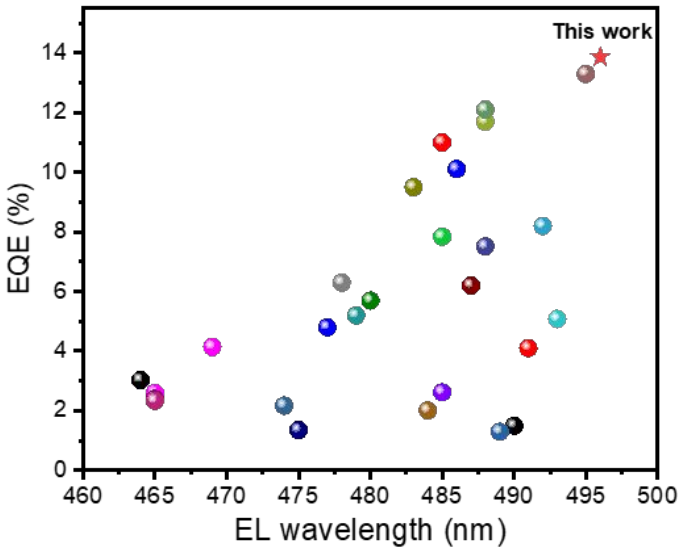

Figure S10. Summary of the EQE of PeLEDs at different emitting wavelength.

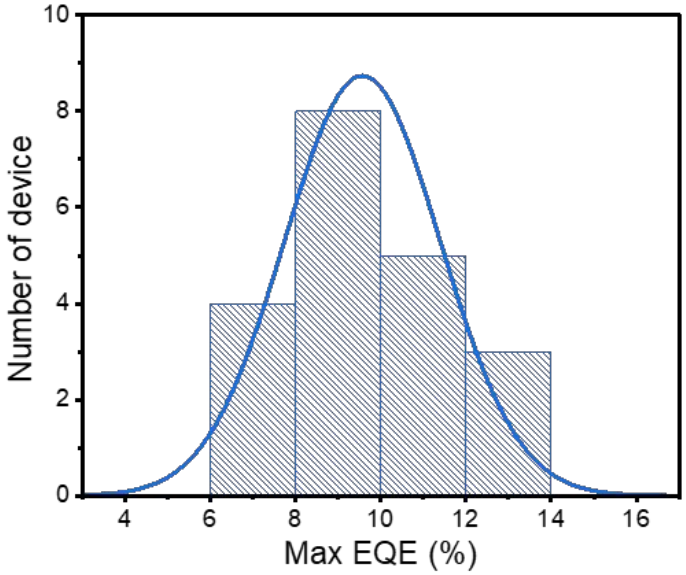

Figure S11. The histogram of EQEs from 20 devices.

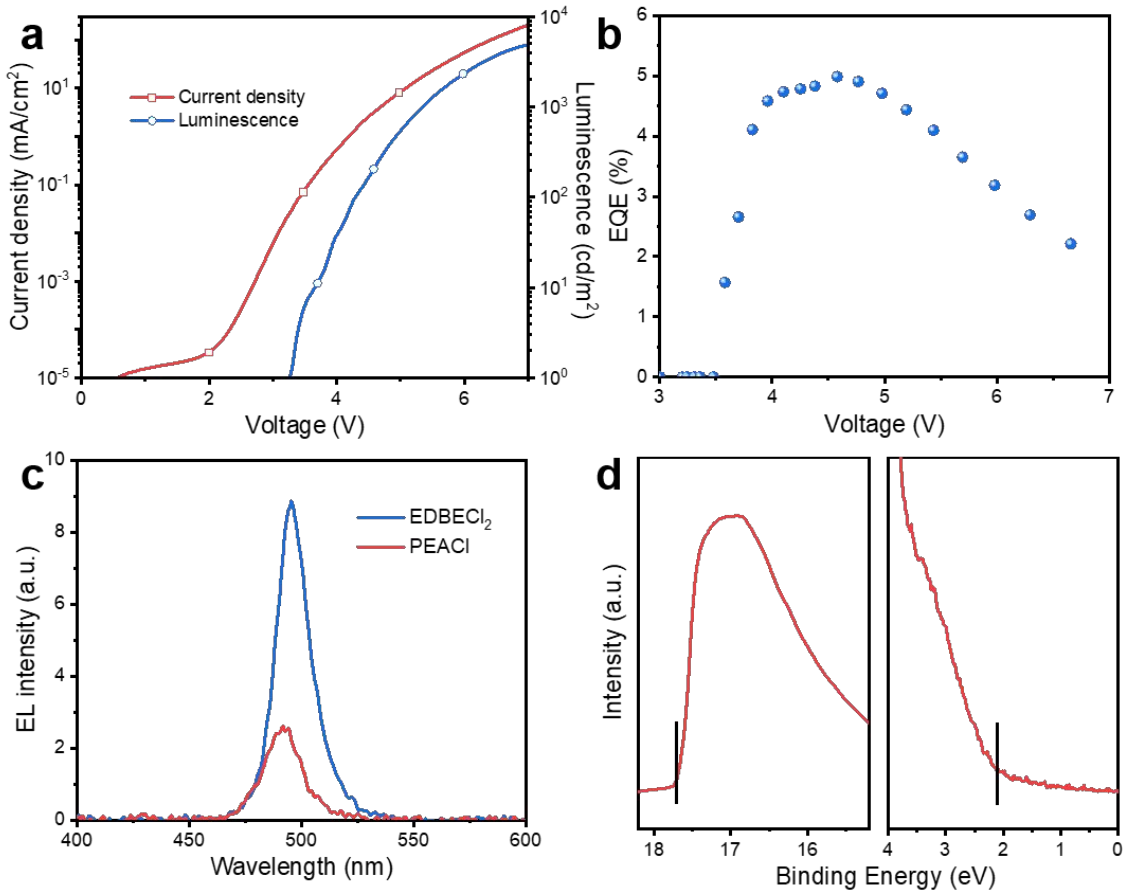

Figure S12. Characterization of PeLED based on PEACl. (a) J-V-L curves. (b) EQE results. (c) Comparison in EL spectra between $EDBECl_2$- and PEACl-based PeLEDs. (d) UPS spectra of PEACl-based perovskite.

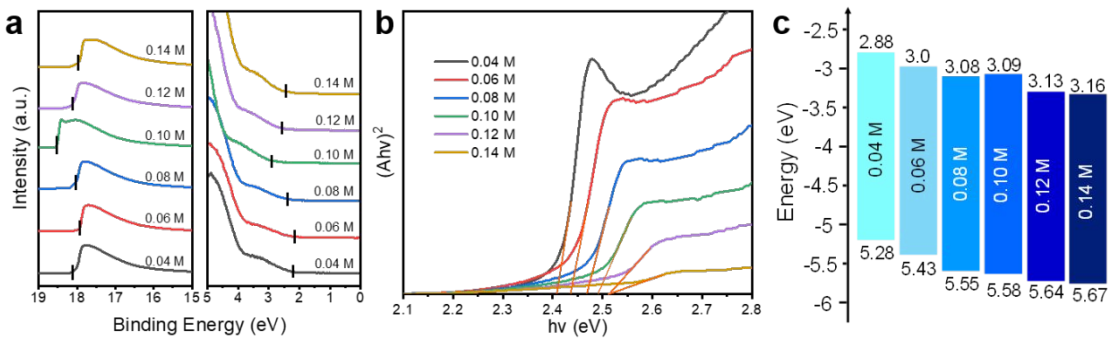

Figure S13. Energy band diagram of perovskites with different $EDBECl_2$ concentrations.

(a) UPS spectra. (b) Tauc plots. (c) Energy diagram.

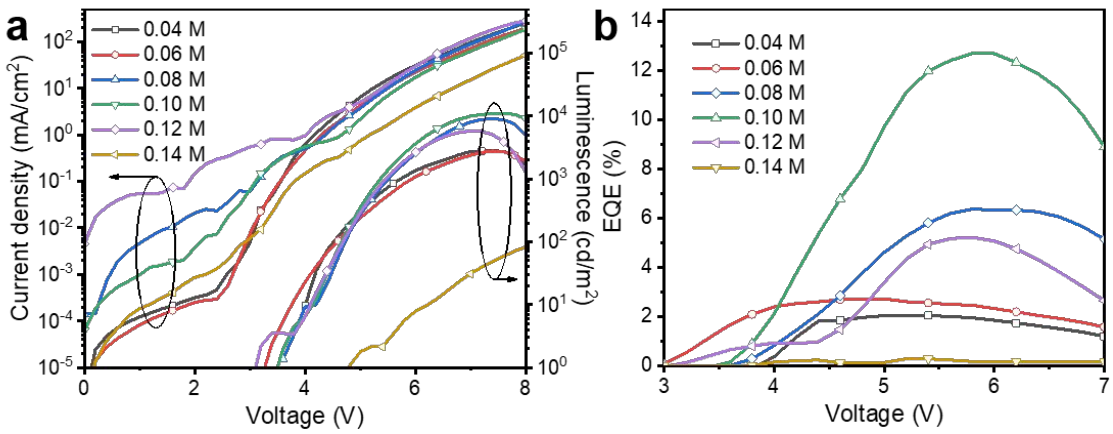

Figure S14. Characterization of PeLEDs with different $EDBECl_2$ concentrations. (a) J-V-L curves. (b) EQE results.

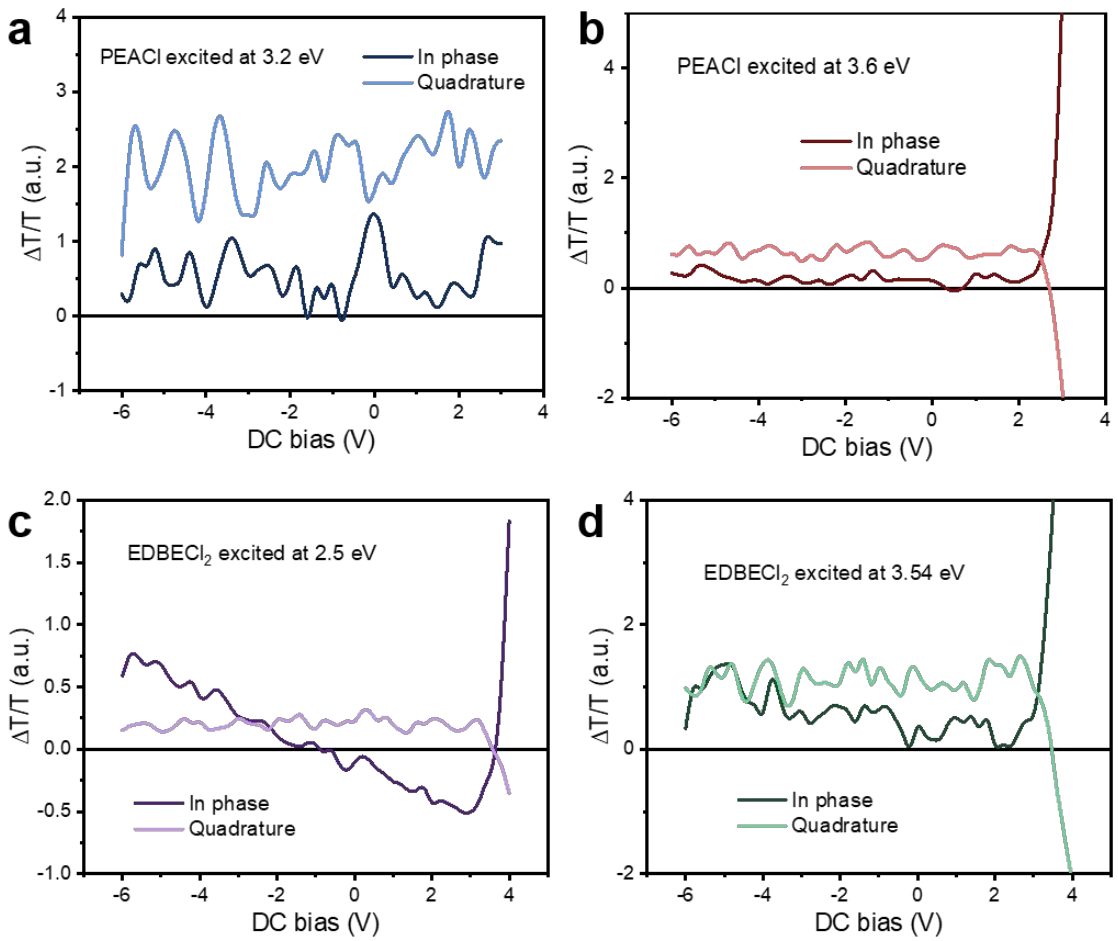

Figure S15. DC voltage dependent CMEAS signals of (a, b) PEACl- and (c, d) $EDBECl_2$-based perovskite excited at different energy.

Supplementary Table

Table S1. Properties of excited states of $EDBECl_2$.

E_{HOMO}/eV	E_{LUMO}/eV	E_g/eV	E_{S1}/eV	E_{T1}/eV
-6.76	-0.33	6.43	5.4340	5.2308

Table S2. Parameters used to calculate hole and electron trap densities. EOD/HOD is short for electron/hole-only device. d is thickness of perovskite layer, n_t is trap density.

	$EDBECl_2$ conc. (M)	V_{TFL} (V)	d (nm)	n_t (10^{17} cm^{-3})
EOD	0.04	2.37	48.3	5.3932
	0.06	2.63	61.9	3.6439
	0.08	2.87	69.6	3.1453
	0.10	2.58	78.6	2.217
	0.12	2.87	89.1	1.9192
	0.14	3.03	99	1.6412
HOD	0.04	2.43	30	14.3338
	0.06	1.92	32.8	9.4744
	0.08	1.76	35	7.6273
	0.10	2.27	40.1	7.4943
	0.12	2.06	43.7	5.7267
	0.14	2.32	47.9	5.368

Table S3. Summary on EL performance of reported blue PeLEDs.

System	EL peak (nm)	EQE_{Max} (%)	L_{Max} (cd m^{-2})	Half lifetime	Ref
$IPA/PEA_2MA/Cs_{n-1}Pb_nBr_{3n-1}$	490	1.5	2480	10 min@10 cd/m^2	Nat. Commun., **2018**, 9, 3541
$PEACl:CsPbBr_3:YCl_3$	485	11	9040	120 min@3.2 V	Nat. Commun., **2019**, 10, 5633
$PEACl:CsPbBr_3:YCl_3$	477	4.8	NA	NA	Nat. Commun., **2019**, 10, 5633
$P\text{-}PDA,PEACs_{n-1}Pb_nBr_{3n+1}$	465	2.6	211	13.5 min@0.35 mA/cm^2	Adv. Mater., **2019**, 31, 1904319
$CsPbCl_{0.9}Br_{2.1}$ with PEA	480	5.7	3780	10 min@4.4 V	Nat. Commun., **2019**, 10, 1027
$PEA_2(Rb_{0.6}Cs_{0.4})_2Pb_3Br_{10}$	475	1.35	100.6	14.5 min @ 4.5 V	Nat. Commun., **2019**, 10, 1868
$PEA_2NPA_1Cs_2Pb_3Br_{12}$	485	2.62	1200	8.8 min@3.0 V	Adv. Funct. Mater., **2020**, 30, 1908339
$BA_2Cs_{n-1}Pbn(Br/Cl)_{3n+1}$	465	2.4	963	NA	Chem. Mater. **2019**, 31, 83−89
$BA_2Cs_{n-1}Pbn(Br/Cl)_{3n+1}$	487	6.2	3339	NA	Chem. Mater. **2019**, 31, 83−89
$PBABr_y(Cs_{0.7}FA_{0.3}PbBr_3)$	483	9.5	54	4.2 min@100 cd/m^2	Nat. Photonics, **2019**, 13, 760-764
DPPOCl treated $PEA_2Cs_{1.6}MA_{0.4}Pb_3Br_{10}$	489	1.3	5141	51 min at 1500 cd/m^2	J. Am. Chem. Soc., **2020**, 142, 5126–5134
DPPOCl treated $PEA_2Cs_{1.6}MA_{0.4}Pb_3Br_{10}$	479	5.2	468	90 min@100 cd/m^2	J. Am. Chem. Soc., **2020**, 142, 5126–5134
$(Cs/Rb/FA/PEA/K)Pb(Cl/Br)_3$	484	2.01	4015	300 min@80 cd/m^2	ACS Energy Lett., **2020**, 5, 1062–1069
$(BA_XPEA_{1-x})_2Cs_{n-1}Pb_n(Br_{0.7}Cl_{0.3})_{3n+1}$	485	7.84	1130	5.2 min@100 cd/m^2	Small, **2020**, 16, 2002940
$(PBA/PEA)_2(MA/FA/Cs)_{n-1}Pb_nBr_{3n+1}$	465	2.34	144.9	NA	ACS Energy Lett., **2020**, 5, 1593−1600
$(PBA/PEA)_2(MA/FA/Cs)_{n-1}Pb_nBr_{3n+1}$	493	5.08	1151	4.2 min@12 cd/m^2	ACS Energy Lett., **2020**, 5, 1593−1600
$PEA_xPA_{2-x}(CsPbBr_3)_{n-1}PbBr_4$	488	7.51	1765	3961 s@1.5 mA/cm^2	ACS Energy Lett., **2020**, 5, 2569−2579
NaBr modified $PEABr_x(CsPb(Cl/Br)_3)$	488	11.7	1511	~560 s@100 cd/m^2	ACS Nano **2020**, 14, 11420−11430
GABA treated $PEA_2Cs_{n-1}Pb_nBr3_{n+1}$	478	6.3	200	150 s@200 cd/m^2	Nat. Commun., **2020**, 11, 3674
$PEA_2(CsPbBr_3)_{n-1}PbBr_4$ with EABr	495	13.3	2790	~230 s@0.35 mA/cm^2	Nat. Commun., **2020**, 11, 4165
$PEA_2(CsPbBr_3)_{n-1}PbBr_4$ with EABr	488	12.1	2191	NA	Nat. Commun., **2020**, 11, 4165
GABr incorporated 2D/3D perovskite	492	8.2	1003	274 s@21 cd/m^2	Adv. Funct. Mater., **2020**, 30, 2001732

$EDABr_2$ substituted $PEA_2CsPb_2Br_7$	474	2.17	290	NA	ACS Appl. Mater. Interfaces **2020**, 12, 45056
DPPACl passivated perovskite	464	3.03	69.4	7 min @5 V	Adv. Funct. Mater., **2020**, 2005553
Sr-substituted perovskite	491	4.1	968	60 min@10 cd/m^2	Adv. Optical Mater., **2020**, 2001073
ABA incorporated quai-2D perovskite	486	10.11	513	81.3 min@ 0.3 mA/cm^2	Adv. Mater., **2020**, 2005570
K modified interface between HTL and perovskite	469	4.14	451	14.0 min@ 1.0 mA/cm^2	Adv. Funct. Mater., **2020**, 2006736
$EDBECl_2$ treat $CsPbBr_3$	496	13.87	2825	26 min@100 cd/m^2	This work

Reference

(1) Tsang, S. W.; Chen, S.; So, F., Energy level alignment and sub-bandgap charge generation in polymer:fullerene bulk heterojunction solar cells. *Adv. Mater.* 2013, 25, 2434-2439.

(2) Campbell, I. H.; Hagler, T. W.; Smith, D. L.; Ferraris, J. P., Direct measurement of conjugated polymer electronic excitation energies using metal/polymer/metal structures. *Phys. Rev. Lett.* 1996, 76, 1900-1903.

(3) Jain, A.; Kumar, P.; Jain, S. C.; Kumar, V.; Kaur, R.; Mehra, R. M., Trap filled limit voltage (VTFL) and V2 law in space charge limited currents. *J. Appl. Phys.* 2007, 102, 094505.

(4) Dong, Y.; Wang, Y. K.; Yuan, F.; Johnston, A.; Liu, Y.; Ma, D.; Choi, M. J.; Chen, B.; Chekini, M.; Baek, S. W.; Sagar, L. K.; Fan, J.; Hou, Y.; Wu, M.; Lee, S.; Sun, B.; Hoogland, S.; Quintero-Bermudez, R.; Ebe, H.; Todorovic, P.; Dinic, F.; Li, P.; Kung, H. T.; Saidaminov, M. I.; Kumacheva, E.; Spiecker, E.; Liao, L. S.; Voznyy, O.; Lu, Z. H.; Sargent, E. H., Bipolar-shell resurfacing for blue LEDs based on strongly confined perovskite quantum dots. *Nat. Nanotechnol.* 2020, 15, 668-674.